


Adaptive line-of-sight path following control for underactuated autonomous underwater vehicles in the presence of ocean currents

Jiangfeng Zeng¹, Lei Wan¹, Yueming Li¹, Zaopeng Dong²
and Yinghao Zhang¹

Abstract

This article presents a nonlinear adaptive line-of-sight path following controller for underactuated autonomous underwater vehicles in the presence of ocean currents. Firstly, a new nonsingular path following error kinematic model in the Serret–Frenet frame is developed, where a nominal course angle error is introduced to significantly simplify the guidance law design. Secondly, an adaptive line-of-sight guidance law with the introduction of the current observer is proposed to make the vehicle produce a variable sideslip angle to compensate for the drift force for any parametric curved-path path following. Benefit from the global κ -exponential convergence property of the designed current observer, the actual course angle error can be eliminated indirectly. Then, dynamic controller built on Lyapunov theory and backstepping technique guarantee the uniform global exponential stability of the yaw and relative surge velocity. In the end, stability analysis shows that the global κ -exponential stability is achieved for the closed-loop system. Simulation results demonstrate the effectiveness of the proposed control scheme.

Keywords

Underactuated autonomous underwater vehicles, path following, line-of-sight guidance, adaptive control, ocean current estimation

Date received: 30 March 2017; accepted: 13 November 2017

Topic: Special Issue—Underwater Environmental Perception and Manipulation

Topic Editor: Professor Andrey V Savkin

Associate Editor: Hai Huang

Introduction

Unmanned marine vehicles are particularly useful in a variety of activities, such as, oil exploration, undersea cables inspection, environmental monitoring, and seabed mapping.^{1–4} Marine vehicles involved in these activities usually execute path following operations. In particular, autonomous underwater vehicles (AUVs) have a major advantage than unmanned surface vehicles (USVs) and remotely operated vehicles (ROVs), when the task is performed in deep waters. However, most AUVs are underactuated and the main environment disturbance ocean current is inevitable, precise path following is challenged.

In path following control scenario, a vehicle is required to follow a predefined path without temporal constraint.⁵ Specifically, the control objective can be described as a

¹ Science and Technology on Underwater Vehicle Laboratory, Harbin Engineering University, Harbin, China

² School of Transportation, Wuhan University of Technology, Wuhan, China

Corresponding authors:

Yueming Li and Jiangfeng Zeng, Science and Technology on Underwater Vehicle Laboratory, Harbin Engineering University, Harbin, 150001 China. Emails: liyueming@hrbeu.edu.cn; zengjiangfeng@hrbeu.edu.cn



force the vehicle to pursue a virtual target point along the path. Since the depth-pitch control of AUVs is usually decoupled from the horizontal plane, most path following control is limited on two-dimensional (2-D) path. In this case, it has something in common with USVs and surface vessels. In recent two decades, various research results have been presented focused on the virtual target-based path following control of AUVs and other marine vehicles, for instance.^{5–9} Encarnação et al.⁵ addressed the path following control of an autonomous marine craft in the Serret–Frenet frame and designed a local path following controller. Using Lyapunov direct method and backstepping technique, a nonsingular path following control law for AUVs was proposed by Lapierre et al.⁶ Considering both the fully-actuated and under-actuated configurations, a novel nonlinear path following controller for fully-actuated/under-actuated AUV was presented by Xiang et al.⁷ Lekkas et al.⁸ investigated both the path planning problem and the guidance problem for marine vehicles by introducing a variation of the cubic Hermite spline interpolation (CHSI) technique and a new integral line of sight (ILOS) algorithm. Using the Nussbaum gain method, a path following controller for underactuated underwater vehicle with inputs constraint was developed by Qi.⁹ It is noted that if the virtual target on the path is chosen to be the nearest reference point, the initial cross-track error should be restricted to be smaller than the smallest radius of the path curvature. This singular problem existed in the literatures.^{5,8} A better solution to relax the initial condition constraints of path following is to select the reference point to be an arbitrary point on the path which will result in the addition of the along-track error.^{6,7,9}

Guidance law is of critical importance that determines the overall performance of the controller during the path following. The LOS method is an effective and popular way to design the guidance law.^{10–16} It has proven to be uniform global asymptotic stability (UGAS) and uniform local exponential stability (ULES).¹⁰ Note that the original LOS guidance law ignored the environmental disturbances and is actually a kind of proportional guidance method. Meanwhile, this LOS guidance law is mainly used for straight line path following. To handle the constant ocean current disturbance in straight line path following, an ILOS guidance was first proposed by Børhaug et al.¹¹ and improved by Caharija et al.¹² Børhaug et al.¹¹ described the dynamics of the marine vehicle by both the absolute velocities and the relative velocities. This makes the controller complex and the system stability weakened. This drawback was removed by Caharija et al.,¹² using the relative velocities of the vehicle. Later, the ILOS was extended to three-dimensional straight line path following for AUVs¹³ and for underwater snake robots.¹⁴ However, this ILOS guidance law was not suitable for curved-path path following since the desired heading angle will not change when the cross-track error is eliminated. Therefore, it is necessary to modify the LOS guidance law that applies to

curved path. Recently, an adaptive LOS (ALOS) guidance principle was proposed by Fossen et al.¹⁵ However, the sideslip angle to be estimated was assumed to be small and constant, and the guidance law was mainly used for Dubins paths. Under the assumption that the path-tangential angle of the desired path varies slowly, an improved adaptive ILOS guidance law was developed by Zheng et al.¹⁶

Environmental disturbances induced by ocean currents, wind, and waves have critical impact on the motion of marine vehicles.¹⁷ In particular, ocean current is the main ingredient of the disturbances for underwater vehicles. So far, most ocean current research results on marine vehicles are under the assumption that the current is irrotational and constant.^{5,11–14,18} Under this assumption, the model of the marine vehicle can be described by the relative velocities, which makes the controller design convenient that can be seen by reviewing Caharija et al.¹² If the ocean current is unknown, current observers are useful in controller design, such as, path following, way-point tracking, and position tracking control.^{5,19–21} These current observers were designed based on the kinematic equations of the vehicle, and the position estimation can be obtained simultaneously. In addition to these observers, the ILOS guidance law also provided a current estimation method by using the steady-state integral term and the relevant velocities.¹² Instead of estimating the current directly, Fossen et al.¹⁵ proposed an adaptation law to estimate the vehicle sideslip angle to compensate for the drift force caused by ocean currents. This method adopted absolute velocities and was mainly used for marine surface vehicles.

Motivated by the above considerations, this article addresses the precision improvement of 2-D curved-path path following control for underactuated AUVs exposed to ocean currents. The current is assumed to be irrotational, constant, and unknown. Considering the current disturbance, a new path following error kinematic model with an amendment to the definition of the course angle error in Serret–Frenet frame is first proposed. Based on it, we propose a new ALOS guidance law which comprises a current estimator. With this guidance law, the vehicle can sideslip to compensate for the drift force. Since the position track errors and the current estimation errors are proven global κ -exponentially converge to zero. The actual course angle error are shown to be eliminated indirectly. Using Lyapunov direct method and backstepping technique, the yaw and relative surge velocity can be controlled simultaneously. Stability analysis shows that the closed-loop system has the stronger stability property of global κ -exponential stability.

To this end, this article makes the following contributions: (1) The new path following error kinematic model developed in this article takes into account the current influence, which is the extension of the model presented by Lapierre et al.⁶ (2) The nominal course

angle error introduced in this article significantly simplify the guidance law design. Meanwhile, the proposed adaptive LOS guidance law can provide AUV with a variable sideslip angle and an accurate current estimation during the path following. (3) The drift angle in this article is not assumed to be small or constant, the guidance law is suitable for curved path with arbitrary curvature not just straight line or circular paths. (4) In the end, this article presents an explicit analysis of the steady state of the AUV in curved-path path following and proves the validity of the introduction of the nominal course angle error.

The rest of this article is organized as follows: “Problem formulation” section presents the path following error kinematics and the control objective. “The path following control system” section proposes an ALOS guidance law and designs the dynamic controller of the vehicle. Meanwhile, the stability analysis of the control system is given. In the section “Simulation results and discussion,” simulation results are provided to illustrate the proposed control method. “Conclusion” section concludes this article.

Problem formulation

In this section, considering the current disturbance, the kinematic and dynamic equations of the underactuated AUV are described in relative velocity form. Then, a new path following error kinematic model in the Serret–Frenet frame is presented. In the end, the control objective is formulated.

Model of the AUV

To study the AUV motion on horizontal plane, the motions of heave, pitch, and roll are neglected. Let the vector $\boldsymbol{\eta} = [x, y, \psi]^T$ denote the position and yaw angle of the vehicle defined in the inertial frame $\{n\}$. Let the vector $\mathbf{v} = [u, v, r]^T$ be the velocities of the vehicle described in the body frame $\{b\}$, where u and v are the surge and sway velocities, respectively, and r is the yaw rate. Then, the absolute linear velocity vector of the vehicle in $\{n\}$ is $\mathbf{V}_t = [\dot{x}, \dot{y}]^T$. Its magnitude is $V_t = \|\mathbf{V}_t\| = \sqrt{\dot{x}^2 + \dot{y}^2} = \sqrt{u^2 + v^2}$ and its direction is $\psi_w = \psi + \beta$ called the course angle, where $\beta = \arctan(v, u)$ is the drift angle. With these notations, the kinematic equations of the AUV with absolute velocities in vector form are

$$\dot{\boldsymbol{\eta}} = \mathbf{R}(\psi)\mathbf{v} \quad (1)$$

$$\mathbf{R}(\psi) = \begin{bmatrix} \cos(\psi) & -\sin(\psi) & 0 \\ \sin(\psi) & \cos(\psi) & 0 \\ 0 & 0 & 1 \end{bmatrix} \quad (2)$$

where the matrix $\mathbf{R}(\psi)$ is the transform matrix from $\{b\}$ to $\{n\}$. In addition, the matrix \mathbf{R} satisfies $\mathbf{R}\mathbf{R}^T = \mathbf{R}^T\mathbf{R} = \mathbf{I}$

and $\det \mathbf{R} = 1$. Consequently, \mathbf{R} is an element in $SO(3)$, which is the special orthogonal group of order 3.²²

Define the ocean current velocity vector as $\mathbf{V}_c = [V_{cx}, V_{cy}]^T$ and its direction as β_c in $\{n\}$. Then, we have $V_{cx} = V_c \cos \beta_c$ and $V_{cy} = V_c \sin \beta_c$, where V_c is the current speed that is $V_c = \|\mathbf{V}_c\| = \sqrt{V_{cx}^2 + V_{cy}^2}$. The current also can be expressed as $\mathbf{v}_c = [u_c, v_c, 0]^T$ in $\{b\}$, and it meets

$$\mathbf{v}_c = \mathbf{R}^T(\psi)[V_{cx}, V_{cy}, 0]^T \quad (3)$$

where $\mathbf{R}^T(\psi)$ is the transform matrix from $\{n\}$ to $\{b\}$. Therefore, the relative velocity of the vehicle with respect to current in $\{b\}$ is $\mathbf{v}_r = [u_r, v_r, r]^T = \mathbf{v} - \mathbf{v}_c$. Similarly, the relative velocity expressed in $\{n\}$ is $\mathbf{V}_r = \mathbf{V}_t - \mathbf{V}_c$. Its norm is $V_r = \|\mathbf{V}_r\| = \sqrt{u_r^2 + v_r^2}$ and the direction is $\psi_r = \psi + \beta_r$, where $\beta_r = \arctan(v_r, u_r)$ is the relative velocity drift angle. The ocean current and the relative velocities in this article are considered to satisfy the following assumptions.

Assumption 1. The current is constant, irrotational and its speed is bounded by a constant $V_{c\max}$ that is $\dot{\mathbf{V}}_c = \mathbf{0}$ and $0 < V_c \leq V_{c\max}$.

Assumption 2. The magnitude of the relative velocity of the AUV is positive, bounded and larger than that of the current velocity such that $0 < V_{r\min} \leq V_r \leq V_{r\max}$ and $V_{c\max} < V_{r\min}$.

Remark 1. When in normal operation, the AUV moves faster than the current. Furthermore, for most AUVs, their speeds are designed to reach much more than 5 m/s and the current speeds are usually less than 1 m/s. Therefore, Assumption 2 is easy to meet for most AUVs. Similar assumptions for other marine vehicles can be seen in the literatures Lekkas et al.²³ and Fossen et al.²⁴

Then, the kinematics of the vehicle expressed by the relative velocities and the current velocities in vector and component forms are

$$\dot{\boldsymbol{\eta}} = \mathbf{R}(\psi)\mathbf{v}_r + [V_{cx}, V_{cy}, 0]^T \quad (4)$$

$$\begin{cases} \dot{x} = u_r \cos \psi - v_r \sin \psi + V_{cx} \\ \dot{y} = u_r \sin \psi + v_r \cos \psi + V_{cy} \\ \dot{\psi} = r \end{cases} \quad (5)$$

To simplify the dynamic model of the AUV, the vehicle is assumed to have three planes of symmetry and a neutrally buoyant. The damping terms higher than two order are not considered. Then, according to Fossen,²² the dynamic equations of an AUV in relative velocity form are

$$\mathbf{M}\dot{\mathbf{v}}_r + \mathbf{C}(\mathbf{v}_r)\mathbf{v}_r + \mathbf{D}(\mathbf{v}_r)\mathbf{v}_r = \boldsymbol{\tau} \quad (6)$$

$$\begin{aligned} \mathbf{M} &= \begin{bmatrix} m_{11} & 0 & 0 \\ 0 & m_{22} & 0 \\ 0 & 0 & m_{33} \end{bmatrix}, \\ \mathbf{C}(\mathbf{v}_r) &= \begin{bmatrix} 0 & 0 & -m_{22}v_r \\ 0 & 0 & m_{11}u_r \\ m_{22}v_r & -m_{11}u_r & 0 \end{bmatrix}, \\ \mathbf{D} &= \begin{bmatrix} d_{u_r} & 0 & 0 \\ 0 & d_{v_r} & 0 \\ 0 & 0 & d_r \end{bmatrix} \end{aligned} \quad (7)$$
$$\dot{u}_r = \frac{m_{22}}{m_{11}} v_r r - \frac{d_{u_r}}{m_{11}} u_r + \frac{\tau_u}{m_{11}} \quad (8)$$

$$\dot{v}_r = -\frac{m_{11}}{m_{22}}u_r r - \frac{d_{v_r}}{m_{22}}v_r \quad (9)$$

$$\dot{r} = -\frac{(m_{22} - m_{11})}{m_{33}} u_r v_r - \frac{d_r}{m_{33}} r + \frac{\tau_r}{m_{33}} \quad (10)$$

In order to describe the path following control problem, a local reference frame $\{f\}$ associated with P is built and christened the Serret–Frenet frame,⁶ as shown in Figure 1. The point P is a free reference point or called the ‘virtual target’ on the predefined planar path S to be followed. The path S can be described by the signed curvilinear abscissa s of P or the path variable ϖ . The position of the vehicle’s center of mass Q can be defined as x_e and y_e in $\{f\}$, where x_e is the along-track error and y_e is the cross-track error.

$$\dot{\mathbf{n}}_p = \mathbf{R}(\alpha_p)[V_p, 0, \omega_p]^T \quad (11)$$

Assumption 3. The curvature of the path and the velocity of the reference point on the path to be followed all have constant upper bounds such that $|c_c(s)| < c_{\max}$ and $|\dot{s}| < V_{p\max}$.

For a given vehicle state η and a reference point state η_p , the error vector η_e between the vehicle and the virtual target expressed in $\{f\}$ is

$$\boldsymbol{\eta}_e = [x_e, y_e, \psi - \alpha_p]^T = \mathbf{R}^T(\alpha_p)(\boldsymbol{\eta} - \boldsymbol{\eta}_p) \quad (12)$$

$$\begin{aligned}\dot{\boldsymbol{\eta}}_e &= \dot{\mathbf{R}}^T(\alpha_p)(\boldsymbol{\eta} - \boldsymbol{\eta}_p) + \mathbf{R}^T(\alpha_p)(\dot{\boldsymbol{\eta}} - \dot{\boldsymbol{\eta}}_p) \\ &= \dot{\alpha}_p \mathbf{S}(\alpha_p) \mathbf{R}^T(\alpha_p)(\boldsymbol{\eta} - \boldsymbol{\eta}_p) + \mathbf{R}^T(\alpha_p)(\dot{\boldsymbol{\eta}} - \dot{\boldsymbol{\eta}}_p) \quad (13)\end{aligned}$$
$$\mathcal{S}(\alpha_p) = \begin{bmatrix} 0 & 1 & 0 \\ -1 & 0 & 0 \\ 0 & 0 & 0 \end{bmatrix} \quad (14)$$

Substituting equation (5) and equations (11) to (12) into equation (13) gives

$$\begin{bmatrix} \dot{x}_e \\ \dot{y}_e \\ r - \omega_p \end{bmatrix} = \begin{bmatrix} 0 & \omega_p & 0 \\ -\omega_p & 0 & 0 \\ 0 & 0 & 0 \end{bmatrix} \begin{bmatrix} x_e \\ y_e \\ \psi - \alpha_p \end{bmatrix} + \begin{bmatrix} \cos(\alpha_p) & \sin(\alpha_p) & 0 \\ -\sin(\alpha_p) & \cos(\alpha_p) & 0 \\ 0 & 0 & 1 \end{bmatrix} \begin{bmatrix} u_r \cos(\psi) - v_r \sin(\psi) + V_c \cos\beta_c - V_p \cos(\psi) \\ u_r \sin(\psi) + v_r \cos(\psi) + V_c \sin\beta_c - V_p \sin(\psi) \\ r - \omega_p \end{bmatrix} \quad (15)$$

Since $\bar{\psi}_e = \psi + \beta_r - \alpha_p$, then $\psi - \alpha_p = \bar{\psi}_e - \beta_r$. Using some algebraic computations, the following concise error kinematics of the AUV with the current disturbance is obtained,

$$\begin{bmatrix} \dot{x}_e \\ \dot{y}_e \\ \dot{\bar{\psi}}_e \end{bmatrix} = \begin{bmatrix} c_c(s)\dot{s}y_e - \dot{s} + V_r \cos\bar{\psi}_e + V_c \cos(\beta_c - \alpha_p) \\ -c_c(s)\dot{s}x_e + V_r \sin\bar{\psi}_e + V_c \sin(\beta_c - \alpha_p) \\ r + \dot{\beta}_r - c_c(s)\dot{s} \end{bmatrix} \quad (16)$$

The control objective

Consider an underactuated AUV given by equations (4) and (6). Let the path be described as a planar geometric curve $\mathbf{p}_d = [x_d(\varpi), y_d(\varpi)]^T \in \mathbf{R}^2$ parameterized by a continuous path variable ϖ in $\{n\}$ and the desired surge relative velocity be u_{rd} . The intuitive path following control objective is to derive feedback control laws for surge force τ_u and yaw torque τ_r to make the vehicle's center of mass Q converge to the reference point P , the absolute velocity vector \mathbf{V}_t aligns with the tangent direction of the path, and the surge relative velocity maintains a constant u_{rd} . Note that aligning \mathbf{V}_t with the path tangent direction means $\psi_e = \psi + \beta - \alpha_p = 0$. Whereas, when we choose the relative velocities, β cannot be calculated directly and β_r appears in the equation (16) in place of β . This inspires us to utilize $\bar{\psi}_e$ to approach a modified LOS angle $\psi_{\text{LOS}m}$, while $\psi_e = 0$ can be guaranteed implicitly. The explicit explanation and proof about $\bar{\psi}_e$ and $\psi_{\text{LOS}m}$ will be given in the next section. Therefore, the path following control objective can be modified as

$$\begin{cases} \lim_{t \rightarrow \infty} x_e = 0 \\ \lim_{t \rightarrow \infty} y_e = 0 \\ \lim_{t \rightarrow \infty} (\bar{\psi}_e - \psi_{\text{LOS}m}) = 0 \\ \lim_{t \rightarrow \infty} (u_r - u_{rd}) = 0 \end{cases} \quad (17)$$

The path following control system

In this section, the guidance-based path following control system is presented. Consider the current is unknown in advance, an ALOS guidance law with a current observer is first proposed. It is suitable for curved path with arbitrary reasonable curvature. The dynamic controller is designed using backstepping technique. In the end, stability analysis

shows that the equilibrium point of the path following error system is global κ -exponential stable.

The ALOS guidance law

In the original LOS guidance law, the heading angle of the vehicle is designed to approach a LOS angle,¹⁰ and it is applicable for straight line path following with no external disturbance. For the integral LOS guidance scheme,¹¹ the heading angle is modified to approach a non-zero LOS angle to compensate for the drift force. However, the integral term will be unchanged when the cross-track error is eliminated, thus it will result in a constant steady LOS angle. This is not reasonable in curved-path path following since the desired heading angle of the vehicle will be variable for different tangent direction angle of the path. Therefore, the desired heading angle should be further modified to adapt to curved path. Considering the AUV model (4), (6), and the path following error kinematics (16) are described in relative velocity form, the desired heading angle ψ_d can be designed as

$$\psi_d = -\beta_r + \alpha_p + \psi_{\text{LOS}m} \quad (18)$$

Notice that β_r is not equal to β when the vehicle is moving on a curved path in current environment, as illustrated in detail in Figure 2. Thus, we cannot hope $\psi_{\text{LOS}m} \rightarrow 0$ when the path following errors are eliminated. Meanwhile, one can see from equation (18) that $\psi \rightarrow \psi_d$ means $\bar{\psi}_e = \psi + \beta_r - \alpha_p \rightarrow \psi_{\text{LOS}m}$, and this is the reason why we renew the control objective with $\lim_{t \rightarrow \infty} (\bar{\psi}_e - \psi_{\text{LOS}m}) = 0$. Furthermore, utilizing $\bar{\psi}_e$ avoids introducing a more complex function of $\psi - \psi_d$ into the guidance law and the virtual yaw rate control.

Then, the next step is to design the guidance angle in equation (18). Since the ocean current is considered unknown, we define $\boldsymbol{\vartheta}_c = [\vartheta_{cx}, \vartheta_{cy}]^T = [V_{cx}, V_{cy}]^T$ as the current velocity to be estimated. Meanwhile, we define $\hat{\boldsymbol{\vartheta}}_c = [\hat{\vartheta}_{cx}, \hat{\vartheta}_{cy}]^T$ as the adaptive estimate value of $\boldsymbol{\vartheta}_c$ and $\tilde{\boldsymbol{\vartheta}}_c = [\tilde{\vartheta}_{cx}, \tilde{\vartheta}_{cy}]^T = \boldsymbol{\vartheta}_c - \hat{\boldsymbol{\vartheta}}_c$ as the parameter estimation errors. The ALOS guidance law is designed as follows

$$\begin{cases} \psi_{\text{LOS}m} = \arcsin\left(-\frac{k_1 y_e}{\sqrt{y_e^2 + \Delta^2}} + \mu\right) \\ \mu = -\frac{1}{V_r}(\hat{\vartheta}_{cy} \cos\alpha_p - \hat{\vartheta}_{cx} \sin\alpha_p) \end{cases} \quad (19)$$

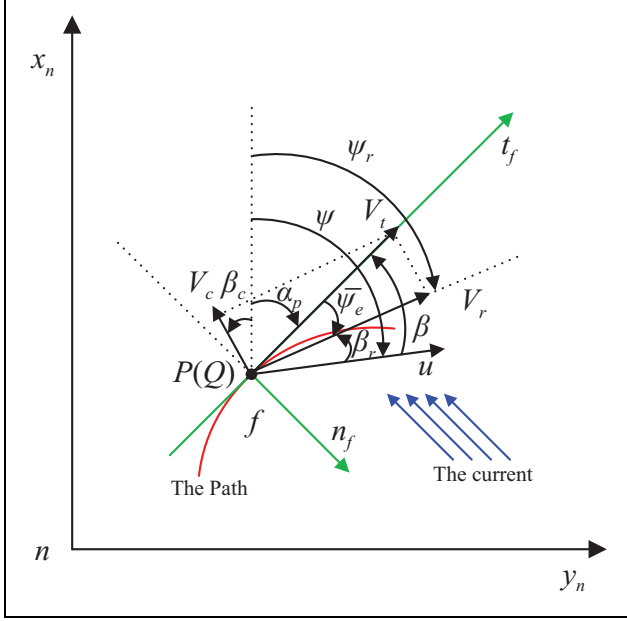


Figure 2. The steady state of the AUV in curved-path path following exposed to ocean current. AUV: autonomous underwater vehicle.

where $k_1 > 0$ is a design parameter, $\Delta > 0$ is the look-ahead distance, and μ is the integral term that creates a variable sideslip angle. In addition, using the inverse rig function $\arcsin(\cdot)$ instead of $\arctan(\cdot)$ is convenient for stability analysis. To estimate the unknown ocean current, the adaptive update law for the current parameters estimation can be designed as

$$\begin{cases} \dot{\hat{\vartheta}}_{cx} = \gamma_c(x_e \cos \alpha_p - y_e \sin \alpha_p) \\ \dot{\hat{\vartheta}}_{cy} = \gamma_c(x_e \sin \alpha_p + y_e \cos \alpha_p) \end{cases} \quad (20)$$

Notice that the hydrodynamic parameters $X_{\dot{u}}$ and $Y_{\dot{v}}$ of AUVs are always negative, and they usually satisfy $X_{\dot{u}} > Y_{\dot{v}}$ if they are stern dominant.²⁵ Thus, there is $\frac{m_{11}}{m_{22}} = \frac{m - X_{\dot{u}}}{m - Y_{\dot{v}}} < 1$, and the yaw rate control equation (25) is well defined.

Remark 3. To derive the guidance law and kinematic controller distinctly, we assume $r = r_d$ and $u_r = u_{rd}$ on the kinematic level. While, the required surge control τ_u and yaw control τ_r will be designed from the dynamic equations in the following subsection.

where $\gamma_c > 0$ is the design parameter.

Remark 2. Combining the current estimation update law (20) and the ALOS guidance law (19), it can be seen that the proposed guidance law is available online in practice since the position track errors x_e and y_e are measurable and the path tangent direction angle α_p is known.

The kinematic controller

As mentioned above, the heading control objective is to stabilize the nominal course angle error $\bar{\psi}_e$ converge to ψ_{LOSm} . Therefore, the evolution of s and the desired yaw rate can be designed as

$$\dot{s} = V_r \cos \bar{\psi}_e + \hat{\vartheta}_{cx} \cos \alpha_p + \hat{\vartheta}_{cy} \sin \alpha_p + k_2 x_e \quad (21)$$

$$r_d = -\dot{\beta}_r + c_c(s)\dot{s} + \dot{\psi}_{LOSm} - k_3(\bar{\psi}_e - \psi_{LOSm}) \quad (22)$$

where k_2 and k_3 are positive control gains. Choose the Lyapunov function candidate (LFC) $V_1 = \frac{1}{2}(\bar{\psi}_e - \psi_{LOSm})^2$. Then, considering equation (22) and $\dot{\bar{\psi}}_e = r_d + \dot{\beta}_r - c_c(s)\dot{s}$, the time derivative of V_1 is

$$\dot{V}_1 = -k_2(\bar{\psi}_e - \psi_{LOSm})^2 \leq -\lambda_1(\bar{\psi}_e - \psi_{LOSm})^2 \quad (23)$$

for some $0 < \lambda_1 < k_2$, which entails that the origin is a UGES equilibrium point.

To acquire a causal form r_d , we make some algebraic computations on $\dot{\beta}_r$. According to the definition of β_r and the vehicle's dynamic equation (9), we have

$$\dot{\beta}_r = -\left[\frac{(m_{11}u_r r + d_v v_r)u_r}{m_{22}} + v_r \dot{u}_r \right] / V_r^2 \quad (24)$$

Then, the virtual control r_d can be calculated as

$$r_d = \left[\dot{\psi}_{LOSm} + \frac{v_r u_r d_v + m_{22} v_r \dot{u}_r}{m_{22} V_r^2} - k_3(\bar{\psi}_e - \psi_{LOSm}) + c_c(s)\dot{s} \right] / \left(1 - \frac{m_{11}}{m_{22}} \cos \beta_r^2 \right) \quad (25)$$

The dynamic controller

The guidance-based path following control scheme treats the kinematic controller as the reference signal to the dynamic control subsystem. While, the errors between the desired values and the actual control outputs can be eliminated on the dynamic level. Using the backstepping technique, the dynamic controller can be designed as

$$\begin{cases} \tau_r = (m_{22} - m_{11})u_r v_r + d_r r + m_{33}\dot{r}_d - m_{33}(\bar{\psi}_e - \psi_{\text{LOS}m}) - k_4 m_{33}(r - r_d) \\ \tau_u = -m_{22}v_r r + d_u u_r - k_5 m_{11}(u_r - u_{rd}) \end{cases} \quad (26)$$

where k_4 and k_5 are arbitrary positive parameters. Define the error variables as

$$\boldsymbol{\varepsilon} = [\varepsilon_r, \varepsilon_{u_r}]^T = [r - r_d, u_r - u_{rd}]^T \quad (27)$$

and choose the LFC as

$$\begin{aligned} V_2 = V_1 + \frac{1}{2}\boldsymbol{\varepsilon}^T \boldsymbol{\varepsilon} &= \frac{1}{2}(\bar{\psi}_e - \psi_{\text{LOS}m})^2 + \frac{1}{2}(r - r_d)^2 \\ &+ \frac{1}{2}(u_r - u_{rd})^2 \end{aligned} \quad (28)$$

Consider the dynamic equations (8) and (10), the virtual yaw rate control equation (22) and the dynamic controller (26), it follows that

$$\begin{aligned} \dot{V}_2 &= (\bar{\psi}_e - \psi_{\text{LOS}m})[\varepsilon_r - k_3(\bar{\psi}_e - \psi_{\text{LOS}m})] \\ &+ (r - r_d)\left[-\frac{(m_{22} - m_{11})}{m_{33}}u_r v_r - \frac{d_r}{m_{33}}r + \frac{\tau_r}{m_{33}} - \dot{r}_d\right] \\ &+ (u_r - u_{rd})\left(\frac{m_{22}}{m_{11}}v_r r - \frac{d_{u_r}}{m_{11}}u_r + \frac{\tau_u}{m_{11}}\right) \\ &= -k_3(\bar{\psi}_e - \psi_{\text{LOS}m})^2 - k_4\varepsilon_r^2 - k_5\varepsilon_{u_r}^2 < 0 \end{aligned} \quad (29)$$

With the similar analysis method of equation (23), we can conclude that the origin

$(\bar{\psi}_e - \psi_{\text{LOS}m}, \varepsilon_r, \varepsilon_{u_r}) = (0, 0, 0)$ is a UGES equilibrium point.

Notice that \dot{r}_d in the first equation (26) implies that the second derivative of β_r is required as seen in equation (22). However, the variable $\ddot{\beta}_r$ is not measurable directly in practice. One solution to this problem is utilizing algebra method based on the dynamics of the AUV and can be carried out as follows:

$$\ddot{\beta}_r = \frac{u_r \ddot{v}_r - v_r \ddot{u}_r}{V_r^2} - 2 \frac{(u_r \dot{v}_r - v_r \dot{u}_r)}{V_r^3} \dot{V}_r = \frac{u_r \ddot{v}_r - v_r \ddot{u}_r}{V_r^2} - 2 \frac{\dot{V}_r}{V_r} \dot{\beta}_r \quad (30)$$

Combining the dynamic control law (26) and the dynamic equations (8) to (10), we have

$$\begin{cases} \ddot{u}_r = k_5^2(u_r - u_{rd}) \\ \ddot{v}_r = -(m_{11}\dot{u}_r r + m_{11}u_r \dot{r} + \dot{d}_{v_r}v_r + d_{v_r}\dot{v}_r)/m_{22} \\ \dot{r} = \dot{r}_d - (\bar{\psi}_e - \psi_{\text{LOS}m}) - k_4(r - r_d) \end{cases} \quad (31)$$

Considering equations (22), (30), and (31), we have

$$\dot{r} = (F_1 + F_2) / \left(1 - \frac{m_{11}}{m_{22}} \cos^2 \beta_r\right) \quad (32)$$

Where

$$\begin{cases} F_1 = \dot{c}_c(s)\dot{s} + c_c(s)\ddot{s} + \ddot{\psi}_{\text{LOS}m} - k_3(\dot{\bar{\psi}}_e - \dot{\psi}_{\text{LOS}m}) - (\bar{\psi}_e - \psi_{\text{LOS}m}) - k_4(r - r_d) \\ F_2 = \frac{u_r}{V_r^2} \left(\frac{m_{11}\dot{u}_r r + \dot{d}_{v_r}v_r + d_{v_r}\dot{v}_r}{m_{22}} \right) + \frac{v_r}{V_r^2} \left[k_5^2(u_r - u_{rd}) \right] + 2 \frac{\dot{V}_r}{V_r} \dot{\beta}_r \end{cases} \quad (33)$$

Then, the dynamic controller can be replaced by

$$\begin{cases} \tau_r = (m_{22} - m_{11})u_r v_r + d_r r + m_{33}(F_1 + F_2) / \left(1 - \frac{m_{11}}{m_{22}} \cos^2 \beta_r\right) \\ \tau_u = -m_{22}v_r r + d_u u_r - k_5 m_{11}(u_r - u_{rd}) \end{cases} \quad (34)$$

Stability analysis of the closed-loop system

Consider the position and the current estimation errors, we define the following LFC

$$V_3 = \frac{1}{2}(x_e^2 + y_e^2) + \frac{1}{2\gamma_c} \tilde{\boldsymbol{\theta}}_c^T \tilde{\boldsymbol{\theta}}_c \quad (35)$$

From equation (16) it follows that

$$\begin{aligned} \dot{V}_3 &= x_e(-\dot{s} + V_r \cos \bar{\psi}_e + \vartheta_{cx} \cos \alpha_p + \vartheta_{cy} \sin \alpha_p) \\ &+ y_e(V_r \sin \bar{\psi}_e + \vartheta_{cy} \cos \alpha_p - \vartheta_{cx} \sin \alpha_p) \\ &+ \frac{1}{\gamma_c} \left(\tilde{\vartheta}_{cx} \dot{\vartheta}_{cx} + \tilde{\vartheta}_{cy} \dot{\vartheta}_{cy} \right) \end{aligned} \quad (36)$$

Since the virtual yaw rate control renders the origin $\bar{\psi}_e - \psi_{\text{LOS}m} = 0$ UGES, we replace $\bar{\psi}_e$ with $\psi_{\text{LOS}m}$ and use the update law of \dot{s} in equation (21). This gives

$$\begin{aligned} \dot{V}_3 = & -k_2 x_e^2 - \frac{k_1 V_r}{\sqrt{y_e^2 + \Delta^2}} y_e^2 + x_e (\tilde{\vartheta}_{cx} \cos \alpha_p + \tilde{\vartheta}_{cy} \sin \alpha_p) \\ & + y_e (\tilde{\vartheta}_{cy} \cos \alpha_p - \tilde{\vartheta}_{cx} \sin \alpha_p) + \frac{1}{\gamma_c} (\tilde{\vartheta}_{cx} \dot{\tilde{\vartheta}}_{cx} + \tilde{\vartheta}_{cy} \dot{\tilde{\vartheta}}_{cy}) \end{aligned} \quad (37)$$

Since $\dot{\tilde{\vartheta}}_{cx} = -\dot{\tilde{\vartheta}}_{cx}$, $\dot{\tilde{\vartheta}}_{cy} = -\dot{\tilde{\vartheta}}_{cy}$, and the current estimation is updated by (20), we have

$$\dot{V}_3 = -k_2 x_e^2 - \frac{k_1 V_r}{\sqrt{y_e^2 + \Delta^2}} y_e^2 \leq 0 \quad (38)$$

Meanwhile, the error system in terms of x_e , y_e , and $\tilde{\boldsymbol{\theta}}_c$ becomes

$$\begin{cases} \dot{x}_e = y_e c_c(s) \dot{s} - k_2 x_e + \tilde{\vartheta}_{cx} \cos \alpha_p + \tilde{\vartheta}_{cy} \sin \alpha_p \\ \dot{y}_e = -x_e c_c(s) \dot{s} - \frac{k_1 V_r}{\sqrt{y_e^2 + \Delta^2}} y_e - \tilde{\vartheta}_{cx} \sin \alpha_p + \tilde{\vartheta}_{cy} \cos \alpha_p \\ \dot{\tilde{\vartheta}}_{cx} = -\gamma_c (x_e \cos \alpha_p - y_e \sin \alpha_p) \\ \dot{\tilde{\vartheta}}_{cy} = -\gamma_c (x_e \sin \alpha_p + y_e \cos \alpha_p) \end{cases} \quad (39)$$

According to the standard Lyapunov arguments, the origin $(x_e, y_e, \tilde{\boldsymbol{\theta}}_c) = (0, 0, \mathbf{0})$ is a uniformly globally stable

equilibrium. With the application of Barbalat's Lemma,²⁶ we can conclude that $(x_e, y_e) \rightarrow (0, 0)$ asymptotically as $t \rightarrow \infty$ and the signals $\tilde{\vartheta}_{cx}$ and $\tilde{\vartheta}_{cy}$ are bounded. However, we are interested in establishing UGAS for all the error variables of system (39). Fortunately, the equilibrium point $(x_e, y_e, \tilde{\boldsymbol{\theta}}_c) = (0, 0, \mathbf{0})$ of equation (39) is shown to be UGAS/ULES (global κ -exponential stable) if we invoke the Theorem 1.²⁷

Theorem 1. For a system in the form of

$$\begin{aligned} \dot{\mathbf{z}}_1 &= \mathbf{h}(\mathbf{z}_1, t) + \mathbf{G}(\mathbf{z}, t) \mathbf{z}_2 \\ \dot{\mathbf{z}}_2 &= -\mathbf{P} \mathbf{G}(\mathbf{z}, t)^T \left(\frac{\partial W(\mathbf{z}_1, t)}{\partial \mathbf{z}_1} \right)^T, \quad \mathbf{P} = \mathbf{P}^T > 0 \end{aligned} \quad (40)$$

where $\mathbf{z}_1 \in \mathbf{R}^{n_1}$, $\mathbf{z}_2 \in \mathbf{R}^{n_2}$, and $W : \mathbf{R}^{n_1} \times \mathbf{R}_{\geq 0} \rightarrow \mathbf{R}_{\geq 0}$ is a ℓ^1 function. All the functions are assumed such that the solutions exist and are unique. Then, the system equation (40) is UGAS if the following two assumptions A1 and A2 hold.

Assumption 1. Define $\mathbf{G}_0(\mathbf{z}_2, t) := \mathbf{G}(\mathbf{z}, t)|_{\mathbf{z}_1 \equiv \mathbf{0}}$. Assume that there exist continuous nondecreasing functions $\rho_j : \mathbf{R}_{\geq 0} \rightarrow \mathbf{R}_{\geq 0}$, ($j = 1, 2, 3$) for all $t \geq 0$ and $\mathbf{z} \in \mathbf{R}^{n_1+n_2}$ that satisfies

$$\begin{cases} \max \left\{ \|\mathbf{h}(\mathbf{z}_1, t)\|, \left\| \frac{\partial W(\mathbf{z}_1, t)}{\partial \mathbf{z}_1} \right\| \right\} \leq \rho_1(\|\mathbf{z}_1\|) \|\mathbf{z}_1\| \\ \max \{ \|\mathbf{G}(\mathbf{z}, t)\|, \|\mathbf{G}_0(\mathbf{z}_2, t)\| \} \leq \rho_2(\|\mathbf{z}\|) \\ \max \left\{ \left\| \frac{\partial \mathbf{G}_0(\mathbf{z}_2, t)}{\partial ((\mathbf{z}_2)_i)} \right\|, \left\| \frac{\partial \mathbf{G}_0(\mathbf{z}_2, t)}{\partial t} \right\| \right\} \leq \rho_3(\|\mathbf{z}_2\|), \quad i \in \{1, \dots, n_2\} \end{cases} \quad (41)$$

Furthermore, for each compact set $\mathbf{K} \subset \mathbf{R}^{n_2}$, there exists $b_m > 0$ such that

$$\mathbf{G}_0(\mathbf{z}_2, t)^T \mathbf{G}_0(\mathbf{z}_2, t) \geq b_m \mathbf{I} \quad (42)$$

for all $(\mathbf{z}_2, t) \in \mathbf{K} \times \mathbf{R}_{\geq 0}$.

Assumption 1. The function $W(\mathbf{z}_1, t)$ satisfies

$$\begin{cases} \alpha_1(\|\mathbf{z}_1\|) \leq W(\mathbf{z}_1, t) \leq \alpha_2(\|\mathbf{z}_1\|) \\ \frac{\partial W(\mathbf{z}_1, t)}{\partial t} + \frac{\partial W(\mathbf{z}_1, t)}{\partial \mathbf{z}_1} \mathbf{h}(\mathbf{z}_1, t) \leq -c \|\mathbf{z}_1\|^2 \end{cases} \quad (43)$$

where α_1 and α_2 are class- k_∞ functions and $c > 0$ is a strictly positive real number. Further, the system is ULES if $\alpha_2(z) \propto z^2$ for sufficiently small z .

In order to analyze the stability of equation (39), we rewrite it in the following form

$$\begin{aligned} \begin{bmatrix} \dot{x}_e \\ \dot{y}_e \end{bmatrix} &= \begin{bmatrix} -k_2 & c_c(s) \dot{s} \\ -c_c(s) \dot{s} & -\frac{k_1 V_r}{\sqrt{y_e^2 + \Delta^2}} \end{bmatrix} \begin{bmatrix} x_e \\ y_e \end{bmatrix} \\ &+ \begin{bmatrix} \cos \alpha_p & \sin \alpha_p \\ -\sin \alpha_p & \cos \alpha_p \end{bmatrix} \begin{bmatrix} \tilde{\vartheta}_{cx} \\ \tilde{\vartheta}_{cy} \end{bmatrix} \end{aligned} \quad (44)$$

$$\begin{bmatrix} \dot{\tilde{\vartheta}}_{cx} \\ \dot{\tilde{\vartheta}}_{cy} \end{bmatrix} = -\gamma_c \begin{bmatrix} \cos \alpha_p & -\sin \alpha_p \\ \sin \alpha_p & \cos \alpha_p \end{bmatrix} \begin{bmatrix} x_e \\ y_e \end{bmatrix} \quad (45)$$

Denote $\mathbf{z}_1 = [x_e, y_e]^T$ and $\mathbf{z}_2 = [\tilde{\vartheta}_{cx}, \tilde{\vartheta}_{cy}]^T$, then

$$\begin{aligned}
\mathbf{P} = \gamma_c, \mathbf{h}(\mathbf{z}_1, t) &= \begin{bmatrix} -k_2 & c_c(s)\dot{s} \\ -c_c(s)\dot{s} & -\frac{k_1 V_r}{\sqrt{y_e^2 + \Delta^2}} \end{bmatrix} \begin{bmatrix} x_e \\ y_e \end{bmatrix} \\
&= \begin{bmatrix} -k_2 x_e + c_c(s)\dot{s} y_e \\ -c_c(s)\dot{s} x_e - \frac{k_1 V_r}{\sqrt{y_e^2 + \Delta^2}} y_e \end{bmatrix} \quad (46) \\
\mathbf{G}(\mathbf{z}, t) &= \begin{bmatrix} \cos \alpha_p & \sin \alpha_p \\ -\sin \alpha_p & \cos \alpha_p \end{bmatrix}, W(\mathbf{z}_1, t) = \frac{1}{2}(x_e^2 + y_e^2) \quad (47)
\end{aligned}$$

Consider assumption 2 and assumption 3, we have that $\frac{V_r}{\sqrt{y_e^2 + \Delta^2}} \leq \frac{V_{r\max}}{\Delta}$ is bounded and $c_c(s)\dot{s}$ is also bounded. Meanwhile, $\frac{\partial W(\mathbf{z}_1, t)}{\partial \mathbf{z}_1} = [x_e, y_e]$ and $\mathbf{G}^T \mathbf{G} = \mathbf{I}_{2 \times 2}$ that is persistently exciting (PE), then assumption A1 holds. We can also check that

$$\begin{aligned}
\frac{\partial W(\mathbf{z}_1, t)}{\partial \mathbf{z}_1} \mathbf{h}(\mathbf{z}_1, t) &= [x_e, y_e] \begin{bmatrix} -k_2 x_e + c_c(s)\dot{s} y_e \\ -c_c(s)\dot{s} x_e - \frac{k_1 V_r}{\sqrt{y_e^2 + \Delta^2}} y_e \end{bmatrix} \\
&= -k_2 x_e^2 - \frac{k_1 V_r}{\sqrt{y_e^2 + \Delta^2}} y_e^2 \quad (48)
\end{aligned}$$

which implies that assumption A2 is also satisfied. Therefore, the system equations (44) and (45) is UGAS. In addition, if we choose $\alpha_2(\|\mathbf{z}_1\|) = 2W(\mathbf{z}_1, t) = x_e^2 + y_e^2$, for all $\mathbf{z}_1 \in \mathbf{R}^2$, then ULES is obtained. Thus, we have proven that the origin of the system (44) and (45) is UGAS/ULES or called global κ -exponential stable.

Moreover, under the above ALOS guidance law and kinematic controller, the actual course angle error ψ_e is indirectly eliminated which is proven in theorem 2.

Theorem 2. Consider an AUV following an arbitrary curved path in the presence of unknown constant ocean current. Assume that the nominal course angle error $\bar{\psi}_e = \psi_{\text{LOS}m}$ is achieved, and the position track errors x_e and y_e and the current estimation errors \tilde{v}_{cx} and \tilde{v}_{cy} all converge to zero, then the actual course angle error $\psi_e = 0$ is guaranteed.

Proof. If the AUV moves in current environment, the velocity vectors \mathbf{V}_r , \mathbf{V}_c , and \mathbf{V}_t meet

$$\mathbf{V}_r + \mathbf{V}_c \equiv \mathbf{V}_t \quad (49)$$

and their geometrical relations are described in Figure 2. Decomposing \mathbf{V}_r and \mathbf{V}_c in the normal direction of \mathbf{V}_t yields

$$V_r \sin(\beta_r - \beta) - V_c \sin(\psi + \beta - \beta_c) = 0 \quad (50)$$

therefore

$$\beta_r - \beta = \arcsin \left[\frac{V_c}{V_r} \sin(\psi + \beta - \beta_c) \right] \quad (51)$$

Consider the ALOS guidance law (19), when the AUV reaches the steady state, that is, $\bar{\psi}_e \rightarrow \psi_{\text{LOS}m}$, $x_e \rightarrow 0$, $y_e \rightarrow 0$, and $\tilde{\boldsymbol{\theta}}_c \rightarrow \mathbf{0}$, it follows

$$\bar{\psi}_e = \psi + \beta_r - \alpha_p = \arcsin \left[-\frac{V_c}{V_r} \sin(\beta_c - \alpha_p) \right] \quad (52)$$

Substituting equation (51) into (52) and replacing $\psi + \beta - \alpha_p$ with ψ_e give

$$\arcsin \left[\frac{V_c}{V_r} \sin(\alpha_p - \beta_c) \right] - \psi_e = \arcsin \left[\frac{V_c}{V_r} \sin(\psi_e + \alpha_p - \beta_c) \right] \quad (53)$$

Utilizing sinusoidal function for both sides of the above equation, and thus

$$\frac{\sin \psi_e}{V_r} \left[V_c \cos(\alpha_p - \beta_c) \pm \sqrt{V_r^2 - V_c^2 \sin^2(\alpha_p - \beta_c)} \right] = 0 \quad (54)$$

According to assumption 2, we have $V_r > V_c > 0$, then

$$\begin{aligned}
|V_c \cos(\alpha_p - \beta_c)| &= \sqrt{V_r^2 - V_c^2 \sin^2(\alpha_p - \beta_c)} \\
&< \sqrt{V_r^2 - V_c^2 \sin^2(\alpha_p - \beta_c)} \quad (55)
\end{aligned}$$

which means that $V_c \cos(\alpha_p - \beta_c) \pm \sqrt{V_r^2 - V_c^2 \sin^2(\alpha_p - \beta_c)}$ will never be equal to zero. Then, equation (54) implies there must be $\sin \psi_e = 0$ namely $\psi_e = 0$ or $\psi_e = \pi$ in a period of 2π . However, $\psi_e = \pi$ means the bow of the AUV is opposite to the path direction which is not reasonable for controllability reasons and will not occur in practice. Therefore, $\psi_e = 0$ is the inevitable result if equation (54) holds. Meanwhile, it is easy to check that when $\psi_e = 0$ equation (54) is always satisfied, which means $\psi_e = 0$ is a sufficient condition. Therefore, $\psi_e = 0$ is indirectly guaranteed, and Theorem 2 has been proven.

To analyze the stability of the closed-loop system, we define the error vector of the system as $\mathbf{x} = [\mathbf{x}_1, \mathbf{x}_2]^T$, where $\mathbf{x}_1 = [x_e, y_e, \tilde{v}_{cx}, \tilde{v}_{cy}]^T$ and $\mathbf{x}_2 = [\bar{\psi}_e - \psi_{\text{LOS}m}, \varepsilon_r, \varepsilon_{ur}]^T$, then the path following error system can be described as

$$\begin{cases} \dot{\mathbf{x}}_1 = f_1(t, \mathbf{x}_1) + g(t, \mathbf{x}) \mathbf{x}_2 \\ \dot{\mathbf{x}}_2 = f_2(t, \mathbf{x}_2) \end{cases} \quad (56)$$

where the interconnection term $g(t, \mathbf{x}) \mathbf{x}_2 = 0$, which can be seen from equations (44) and (45). Then, the cascade system theorem can be used to proof the stability of the system (56). As analyzed above, the subsystem $\sum_1 : \dot{\mathbf{x}}_1 = f_1(t, \mathbf{x}_1)$ is global κ -exponential stable and the

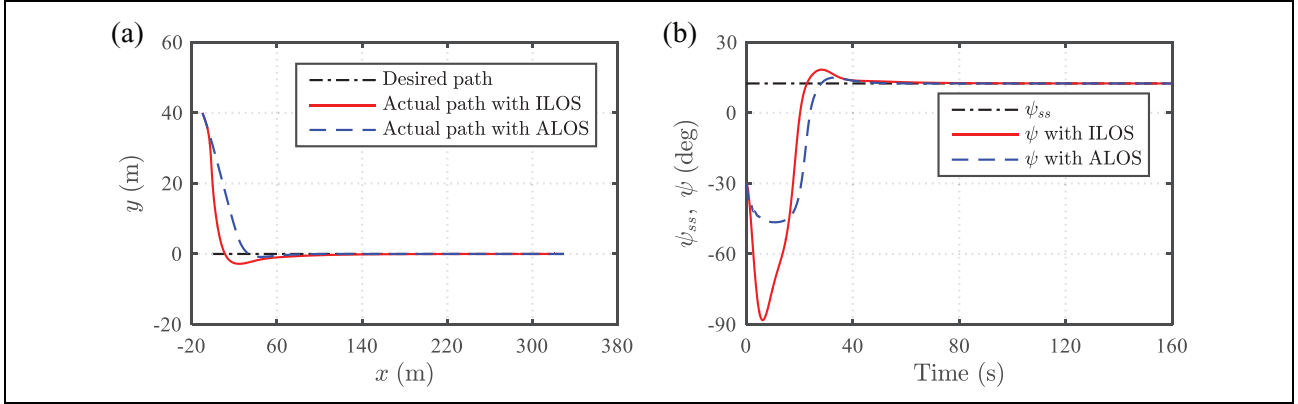


Figure 3. Straight line path following comparison between the ILOS and ALOS approaches: position, steady-state heading angle, and heading angle. ILOS: integral line of sight; ALOS: adaptive line of sight.

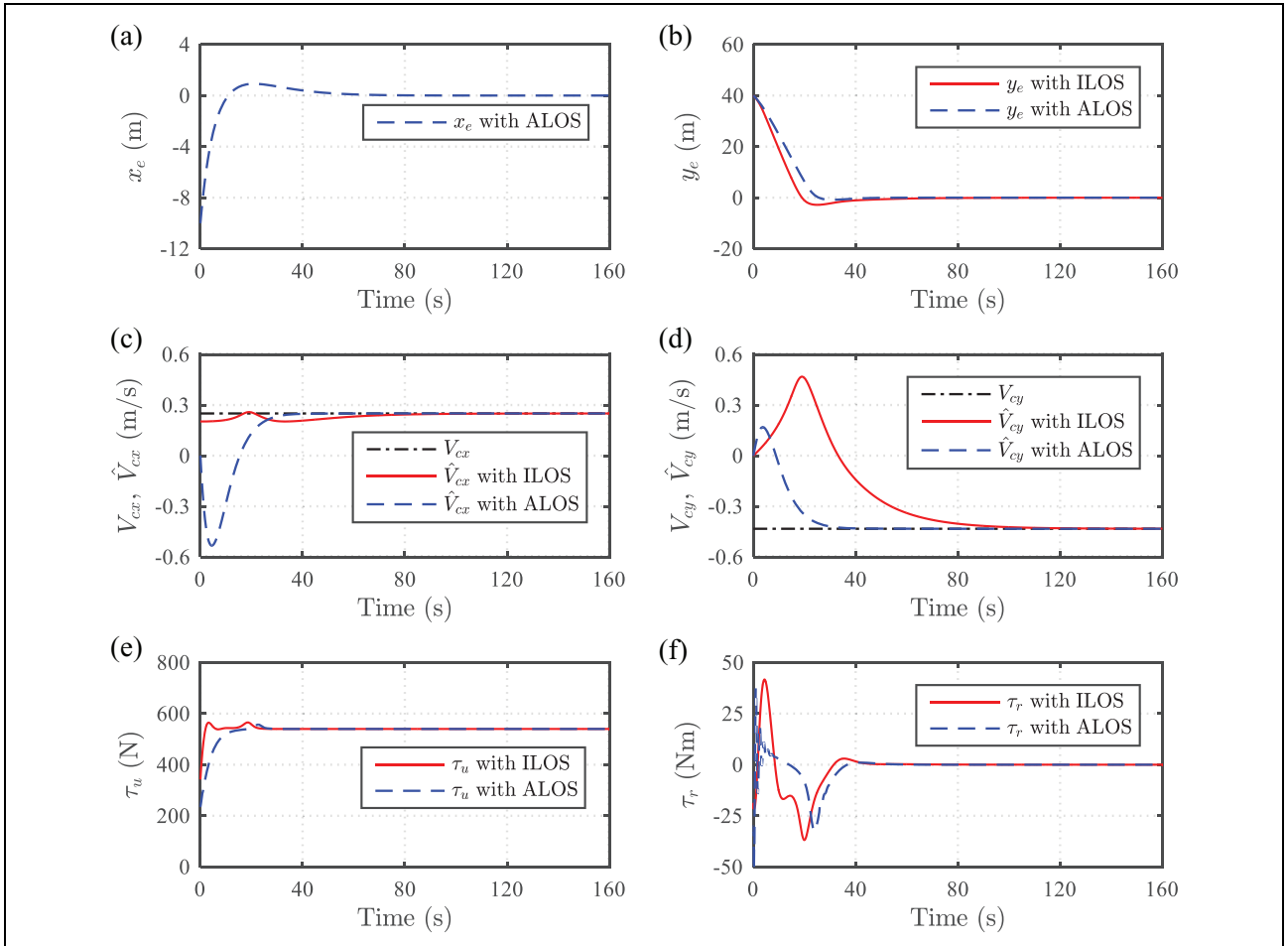


Figure 4. Straight line path following comparison between the ILOS and ALOS approaches: position track errors, current estimations and control inputs. ILOS: integral line of sight; ALOS: adaptive line of sight.

subsystem $\sum_2 : \dot{x}_2 = f_2(t, x_2)$ is UGES. All the three assumptions of Theorem 7 are satisfied.²⁸ Therefore, the system (56) is UGAS. Moreover, we can conclude that the equilibrium point $x = 0$ of the error system (56) is global κ -exponential stable from Lemma 8 of Panteley et al.²⁸

Simulation results and discussion

In this section, numerical simulation results are given to illustrate the performance of the proposed control law and the exponential convergence property of the control system is demonstrated. The considered AUV model was given by

Pettersen et al.²⁵ In straight line path following, it shows a better convergence performance compared with the ILOS control method.¹² For curved-path path following, the AUV is assigned to follow a parametric curved path where the universal applicability and the improvement of precision characteristics are presented.

Straight line path following

The control objective is to make the AUV follow a straight line path parametrized as $x_d(\varpi) = \varpi$, $y_d(\varpi) = 0$ with a

Table I. Parameters of the curved path.

$a_0 = 0$	$a_1 = 0.85$	$a_2 = -0.02$	$a_3 = 10^{-6}$	$a_4 = 1.5 \times 10^{-6}$
$b_0 = 0$	$b_1 = 0.5$	$b_2 = 10^{-3}$	$b_3 = 1.5 \times 10^{-5}$	$b_4 = 8 \times 10^{-8}$

desired relative surge speed $u_{rd} = 2 \text{ m/s}$. The initial states of the AUV are $\boldsymbol{\eta}_0 = [-10, 40, -30^\circ]^T$, $u_{r0} = 1 \text{ m/s}$, and others are zero. The intensity of the ocean current is $V_c = 0.5 \text{ m/s}$ and its direction is $\beta_c = -60^\circ$. The parameters of the guidance law in equations (19) and (20), the evolution of s in equation (21), and the dynamic controller are chosen as $k_1 = 1$, $k_2 = 0.4$, $k_3 = 0.3$, $k_4 = 5$, $k_5 = 0.1$, $\Delta = 4 \text{ m}$, and $\gamma_c = 0.04$, where the values of k_1 , k_2 , and γ_c are a compromise between the position track errors and the current estimation errors convergence rates. Since we can see in equation (39) that increasing k_1 and k_2 will make y_e and x_e reach zero rapidly, while the update of \hat{V}_{cx} and \hat{V}_{cy} needs more information of y_e and x_e . k_3 , k_4 , and k_5 are designed to tune the convergence of ε_r and ε_{u_r} . The value of Δ is chosen to sharp the vehicle moving toward the desired path smoothly. The integral LOS controller is

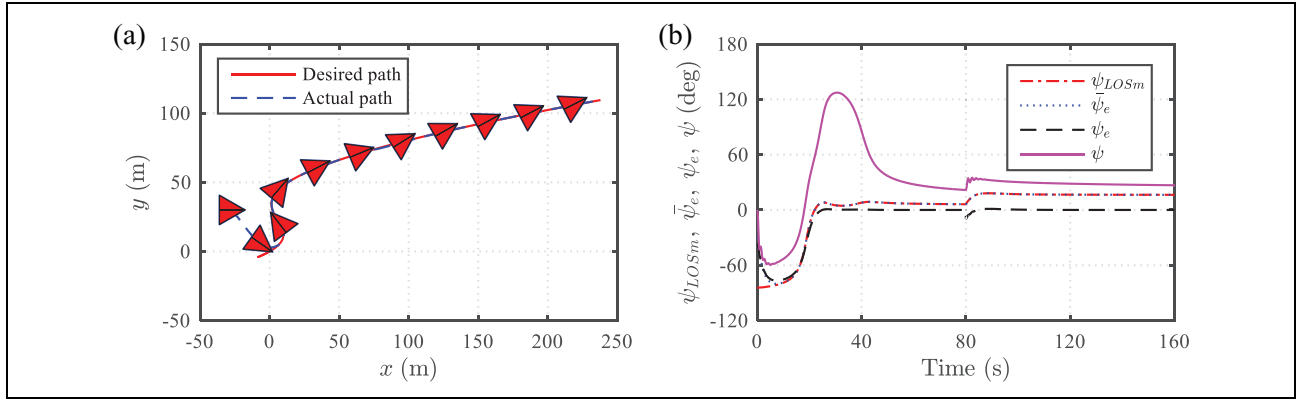


Figure 5. Curved-path path following: position, ALOS angle, nominal course angle error, actual course angle error and heading angle. ALOS: adaptive line of sight.

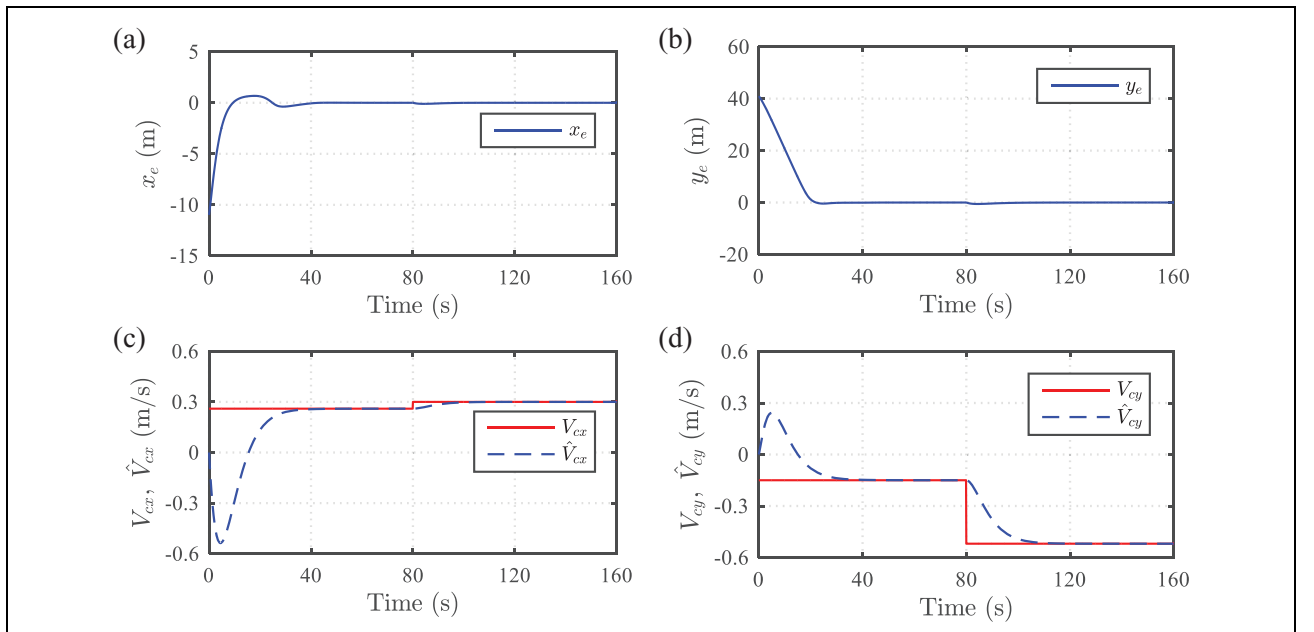


Figure 6. Curved-path path following: position track errors and current estimations.

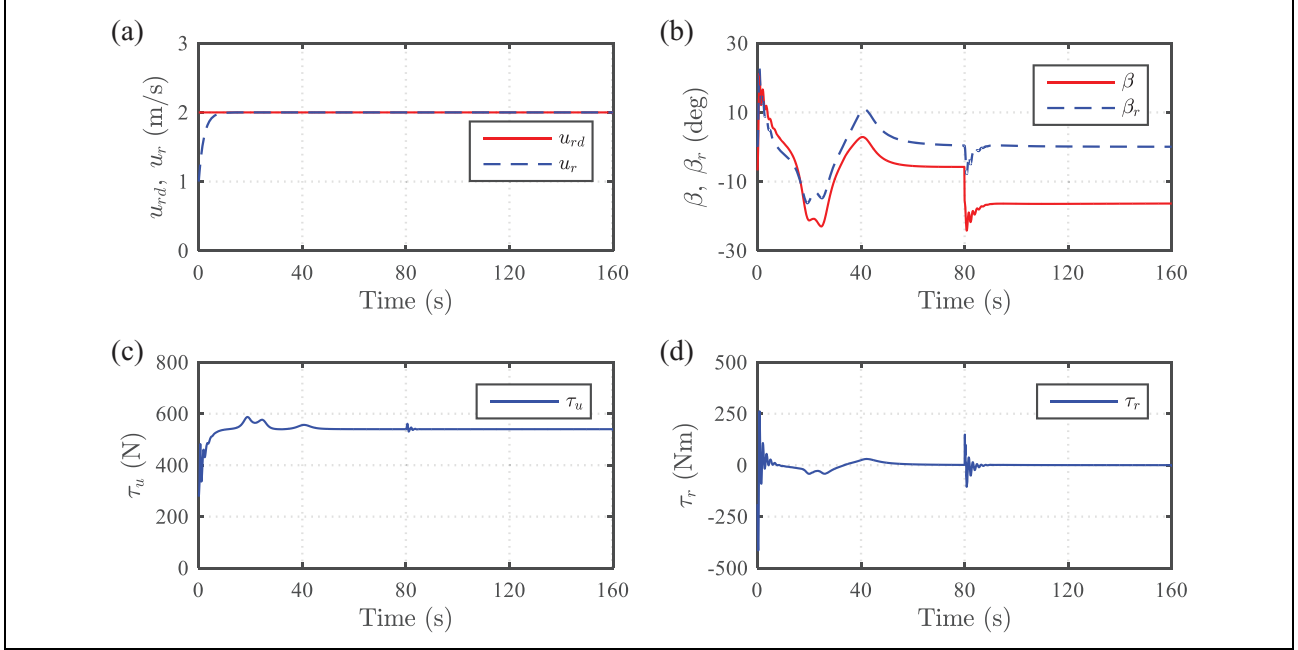


Figure 7. Curved-path path following: relative surge velocity track error, drift angle, relative velocity drift angle and control inputs.

marked as ILOS, and the proposed adaptive LOS controller is marked as ALOS. Simulation results are shown in Figures 3 and 4.

From Figure 3(a) and 4(b), one can see that the ALOS controller has a less overshoot of the cross-track error y_e compared with the ILOS method. Since the ALOS controller solved the singularity problem by using the non-nearest reference point strategy, the along-track error x_e is extra as seen in Figure 4(a) and has a smooth convergence performance. Figure 3(b) shows that the heading angles of the two controllers all achieve the steady-state value $\psi_{ss} \approx 12.5039^\circ$ to compensate for the current force, where the change of ψ with ALOS approach is more gently. The unknown current estimation results are shown in Figure 4(c) and 4(d). Although the ALOS method has larger initial estimation errors, the time to identify the true values of V_{cx} and V_{cy} is less than that of ILOS method. This benefits from the adaptive update law (20). Since the signals x_e , y_e , and α_p are available, the estimation values can be updated online. In the steady state, the vehicle sideslip to compensate for the drift force depended mainly on τ_u , which can be seen from Figure 4(e) and 4(f).

Curved-path path following

The curved path is defined in Cartesian coordinates and parametrized in polynomial form, that is

$$x_d(\varpi) = \sum_{i=0}^4 a_i \varpi^i, y_d(\varpi) = \sum_{i=0}^4 b_i \varpi^i \quad (57)$$

where the path parameters are shown in Table 1.

The desired relative surge velocity is also chosen as $u_{rd} = 2 \text{ m/s}$. The initial states of the AUV are $\eta_0 = [-30, 30, 0^\circ]^T$, $u_{r0} = 1 \text{ m/s}$, and others are zero. The parameters of the control system are chosen the same as that of the straight line path following. To show the robustness of the proposed ALOS control law. The following scenario is considered. In the time $0 \leq t < 80 \text{ s}$, a constant current with speed $V_c = 0.3 \text{ m/s}$ and direction $\beta_c = -30^\circ$ affects the vehicle. While $t \geq 80 \text{ s}$, the current speed increases to $V_c = 0.6 \text{ m/s}$ and the direction becomes $\beta_c = -60^\circ$. Simulation results are shown in Figures 5–7.

From the “red triangular AUV” with heading angle as shown in Figure 5(a), one can intuitively see that the AUV follows the desired curved path perfectly. The position tracking error x_e , y_e all converge to zero and the relative surge velocity u_r approaches to the desired value u_{rd} in the end. After time $t = 80 \text{ s}$, the current force increased and the vehicle deviates slightly from the given path and then returns to the desired position after a short time. Note that although the proposed ALOS guidance law aims to achieve $\psi_e = \psi_{LOSm}$, the actual course angle error ψ_e can be indirectly eliminated which is confirmed in Figure 5(b). Thus, theorem 2 is verified. Figure 6(c) and 6(d) shows how the current observer estimates the unknown constant currents. Though the current changes, it still can be tracked accurately after a transition time. The slight overshoot of the estimation in the initial stage is mainly due to the integral action of the guidance law (19). Thus, γ_c should not be designed too large, otherwise it will cause greater overshoot of the current estimation. Figure 7(b) shows that the guidance law can produce a variable drift angle β to compensate for the drift force. In the time interval $0 \leq t < 80 \text{ s}$, the main contribution to β is the change of the path

curvature $c_c(s)$, while, after time $t = 80s$, a larger drift angle β is generated due to the increase of the current velocity V_c . Therefore, the proposed ALOS guidance law is suitable for any parametric curved path, not just for straight lines or circular paths. Thus, a more precise curved-path path following performance is guaranteed. In the end, one can see that the control inputs τ_u , τ_r shake gently when the current force increased but in reasonable ranges.

Conclusion

An ALOS path following control strategy of underactuated AUVs for current estimation and compensation of the sideslip angle has been presented. The ALOS guidance law is derived based on a new path following error kinematic model with the consideration of the current disturbance. Since the virtual target point is not the nearest reference point, the singularity problem in curved-path path following is resolved. Meanwhile, the drift angle in this article is not assumed to be too small or constant, the proposed path following control strategy is suitable for curved path with arbitrary reasonable curvature, not just straight line and circular paths. Although the proposed ALOS guidance law aims to achieve the convergence of nominal course angle error to the modified LOS angle, the global κ -exponential stability of the position and current estimation error system guarantees that the actual course angle error eliminated indirectly. Lyapunov direct method and backstepping technique are used to design the yaw and the relative surge velocity controllers. Stability analysis shows that the whole control system has the stronger stability property of global κ -exponential stability.

Simulations validate the effectiveness of the proposed control method. Moreover, in straight line path following case, it shows a better tracking performance compared with the previous ILOS guidance law. During curved-path path following scenario, the ALOS guidance law provides a variable sideslip angle to adapt to the currents and path curvature changes. Furthermore, although the proposed control strategy is designed for constant currents, it is able to respond effectively to the step change currents.


Declaration of conflicting interests

The author(s) declared no potential conflicts of interest with respect to the research, authorship, and/or publication of this article.

Funding

The author(s) disclosed receipt of the following financial support for the research, authorship and/or publication of this article: This work was supported by the National Science and Technology Major Project of China (No. 2015ZX01041101) and the National Natural Science Foundation of China (No. 51509057, 51709214).

ORCID iD

Jiangfeng Zeng  <http://orcid.org/0000-0002-4330-2725>

References

1. Mahmoudzadeh S, Powers DMW, and Sammut K. An autonomous reactive architecture for efficient AUV mission time management in realistic dynamic ocean environment. *Rob Auton Syst* 2016; 87: 81–103.
2. Shukla A and Karki H. Application of robotics in offshore oil and gas industry-A review Part II. *Rob Auton Syst* 2015; 75: 508–524.
3. Ludvigsen M and Sørensen AJ. Towards integrated autonomous underwater operations for ocean mapping and monitoring. *Annu Rev Control* 2016; 42: 145–157.
4. Vasilijevic A, Nad D, Mandic F, et al. Coordinated navigation of surface and underwater marine robotic vehicles for ocean sampling and environmental monitoring. *IEEE/ASME Trans Mechatronics* 2017; 22: 1174–1184.
5. Encarnação P, Pascoal A, and Arcak M. Path following for marine vehicles in the presence of unknown currents. In: *SYROCO'2000 6th International IFAC Symposium on Robot Control*, Vienna, Austria, 21–23 September 2000, pp. 469–474. Elsevier IFAC Publications.
6. Lapierre L and Soetanto D. Nonlinear path-following control of an AUV. *Ocean Eng* 2007; 34: 1734–1744.
7. Xiang X, Lapierre L, and Jouvencel B. Smooth transition of AUV motion control: from fully-actuated to under-actuated configuration. *Rob Auton Syst* 2014; 67: 14–22.
8. Lekkas AM and Fossen TI. Integral LOS path following for curved paths based on a monotone cubic hermite spline parametrization. *IEEE Trans Control Syst Technol* 2014; 22: 2287–2301.
9. Qi X. Spatial target path following control based on Nussbaum gain method for underactuated underwater vehicle. *Ocean Eng* 2015; 104: 680–685.
10. Fossen TI, Breivik M, and Skjetne R. Line-of-sight path following of underactuated marine craft. In: *Proceedings of the 6th IFAC MCMC*, Girona, Spain, 17–19 September 2003, pp. 1–6. Elsevier IFAC Publications.
11. Børhaug E, Pavlov A, and Pettersen KY. Integral LOS control for path following of underactuated marine surface vessels in the presence of constant ocean currents. In: *Proceedings of the 47th IEEE Conference on Decision and Control*, Cancun, Mexico, 9–11 December 2008, pp. 4984–4991. New York: IEEE.
12. Caharija W, Pettersen KY, and Sorensen AJ. Relative velocity control and integral line of sight for path following of autonomous surface vessels: merging intuition with theory. *Proc Inst Mech Eng M J Eng Marit Environ* 2014; 228: 180–191.
13. Caharija W, Pettersen KY, Bibuli M, et al. Integral line-of-sight guidance and control of underactuated marine vehicles: theory, simulations, and experiments. *IEEE Trans Control Syst* 2016; 24: 1623–1642.

14. Kelasidi E, Liljebäck P, and Pettersen KY. Integral line-of-sight guidance for path following control of underwater snake robots: theory and experiments. *IEEE Trans Rob* 2017; 33: 610–628.
15. Fossen TI, Pettersen KY, and Galeazzi R. Line-of-sight path following for Dubins paths with adaptive sideslip compensation of drift forces. *IEEE Trans Control Syst Technol* 2015; 23: 820–827.
16. Zheng Z and Sun L. Path following control for marine surface vessel with uncertainties and input saturation. *Neurocomputing* 2016; 177: 158–167.
17. Do KD. Global robust adaptive path-tracking control of underactuated ships under stochastic disturbances. *Ocean Eng* 2016; 111: 267–278.
18. Dong Z, Wan L, Liu T, et al. Horizontal-plane trajectory-tracking control of an underactuated unmanned marine vehicle in the presence of ocean currents. *Int J Adv Robot Syst* 2016; 13: 1–14.
19. Paliotta C and Pettersen KY. Geometric path following with ocean current estimation for ASVs and AUVs. In: *Proceedings of American control conference*, Boston, MA, 6–8 July 2016, pp. 7261–7268. New York: IEEE.
20. Pascoal AM. Dynamic positioning and way-point tracking of underactuated AUVs in the presence of ocean currents. *Int J Control* 2007; 80: 1092–1108.
21. Bi FY, Wei YJ, Zhang JZ, et al. Position-tracking control of underactuated autonomous underwater vehicles in the presence of unknown ocean currents. *IET Control Theory Appl* 2010; 4: 2369–2380.
22. Fossen TI. *Handbook of marine craft hydrodynamics and motion control*. New Jersey: John Wiley & Sons, Inc., 2011.
23. Lekkas AM. *Guidance and path-planning systems for autonomous vehicles*. PhD Thesis, Norwegian University of Science and Technology, Norway, 2014.
24. Fossen TI, Lekkas, and Anastasios M. Direct and indirect adaptive integral line-of-sight path-following controllers for marine craft exposed to ocean currents. *Int J Adapt Control Signal Process* 2017; 31: 445–463.
25. Pettersen KY and Egeland O. Time-varying exponential stabilization of the position and attitude of an underactuated autonomous underwater vehicle. *IEEE Trans Autom Control* 1999; 44: 112–115.
26. Khalil HK. *Nonlinear systems*. 3rd ed. Upper Saddle River, New Jersey, 2002.
27. Fossen TI, Loria A, and Teel A. A theorem for UGAS and ULES of (passive) nonautonomous systems: robust control of mechanical systems and ships. *Int J Robust Nonlinear Control* 2001; 11: 95–108.
28. Panteley E, Lefeber E, Loria A, et al. Exponential tracking control of a mobile car using a cascaded approach. In: *Proceedings of IFAC workshop on motion control*, Grenoble, France, 21–23 September, 1998, pp. 221–226. Elsevier IFAC Publications.